

# Clinical Assessment of Scleral Canal Area in Glaucoma Using Spectral-Domain Optical Coherence Tomography



YU SAWADA, MAKOTO ARAIE, HITOMI SHIBATA, KATSUYUKI MURATA, MAKOTO ISHIKAWA, TAKESHI YOSHITOMI, AND TAKESHI IWASE

- **PURPOSE:** To investigate anterior scleral canal (ASC) area in the eyes with glaucoma using spectral-domain optical coherence tomography (SDOCT).
- **DESIGN:** Cross-sectional study.
- **METHODS:** This study included 206 eyes of 103 patients with glaucoma, classified as 66 eyes of 33 patients with unilateral glaucoma and 140 eyes of 70 patients with bilateral glaucoma. Radial scan enhanced depth imaging SDOCT centered on the optic disc was performed, and parameters that present ASC area such as ASC opening and the largest ASC area were obtained in each eye. The largest ASC area was the largest cross-sectional area of the ASC region identified between the ASC opening and anterior lamina cribrosa insertion. These parameters were compared between eyes with and without glaucoma in unilateral glaucoma, and eyes with worse and better visual field defect (VFD) in bilateral glaucoma.
- **RESULTS:** In the patients with unilateral glaucoma, ASC opening and largest ASC area were significantly larger in the eyes with glaucoma than in those without glaucoma (both  $P < .001$ ). In bilateral glaucoma, these parameters were significantly larger in the eyes with worse VFD than in those with better VFD ( $P = .0080$  and  $P = .0018$ , respectively). Intereye differences of the ASC parameters in the glaucoma patients were significantly greater than that in the normal subjects.
- **CONCLUSIONS:** Significantly larger ASC area was first observed in the living human eyes with glaucoma compared to the normal eyes. Further longitudinal studies are required to determine if the ASC area is useful in the prevention and treatment of glaucoma. (Am J Ophthalmol 2020;216:28–36. © 2020 Elsevier Inc. All rights reserved.)

**E**YES WITH GLAUCOMA PRESENT UNIQUE DEFORMATION of optic nerve head (ONH) including large cupping. Glaucomatous cupping involves deformation and remodeling of the connective tissue of the lamina cribrosa (LC), scleral canal wall, and peripapillary sclera that lead to compression and progressive loss of the neural rim tissue (Figure 1).<sup>1–4</sup> The LC is accepted to be the site of retinal ganglion cell axonal injury in glaucoma,<sup>1,5,6</sup> and numerous studies have been conducted on laminar deformation to date.<sup>5–9</sup> Compared to deformation of the LC, scleral canal deformation has not been studied in much detail, and it was limited mostly to the histologic studies. In human cadaver eyes with glaucoma, the anterior scleral canal (ASC) expanded along with the posterior displacement of the LC.<sup>1,5</sup> In monkey unilateral experimental glaucoma, the ASC expanded in the glaucomatous eyes compared to the fellow normal eyes.<sup>10–12</sup>

A thorough understanding of scleral canal deformation as a part of the entire glaucomatous optic disc deformation process is important, because scleral and laminar deformations are reported to interact.<sup>13–16</sup> This implies that the LC does not respond to the intraocular pressure (IOP) stress in isolation, but scleral deformation may play an important role in the response of the LC to the IOP.

Despite its importance in glaucomatous ONH deformation, to the best of our knowledge, scleral canal deformation has not been investigated in living human eyes to date. One of the reasons for that might be the difficulty in observing deep ONH structures. The recent development of spectral-domain optical coherence tomography (SDOCT) and enhanced depth imaging technique has enabled us to visualize deep ONH structures,<sup>17,18</sup> including ASC opening, which is now used in evaluating the position of the LC and peripapillary choroidal thickness.<sup>19–21</sup> On the basis of the previous histologic studies, we hypothesized that the scleral canal may also be expanded in living human eyes with glaucoma. It may create excavated ONH together with the posteriorly displaced LC and contribute to the glaucomatous axonal damage. Therefore, the purpose of the present study was to examine the ASC area in living human eyes with glaucoma by using SDOCT.

Accepted for publication Mar 31, 2020.

From the Departments of Ophthalmology (Y.S., H.S., M.I., T.I.) and Environmental and Public Health (K.M.), Akita University Graduate School of Medicine, Akita, Japan; Kanto Central Hospital of the Mutual Aid Association of Public School Teachers, Tokyo, Japan (M.A.); and Fukuoka International University of Health and Welfare, Fukuoka, Japan (T.Y.).

Inquiries to Yu Sawada, Department of Ophthalmology, Akita University Graduate School of Medicine, Hondo, Akita 010-8543, Japan; e-mail: sawadayu@doc.med.akita-u.ac.jp

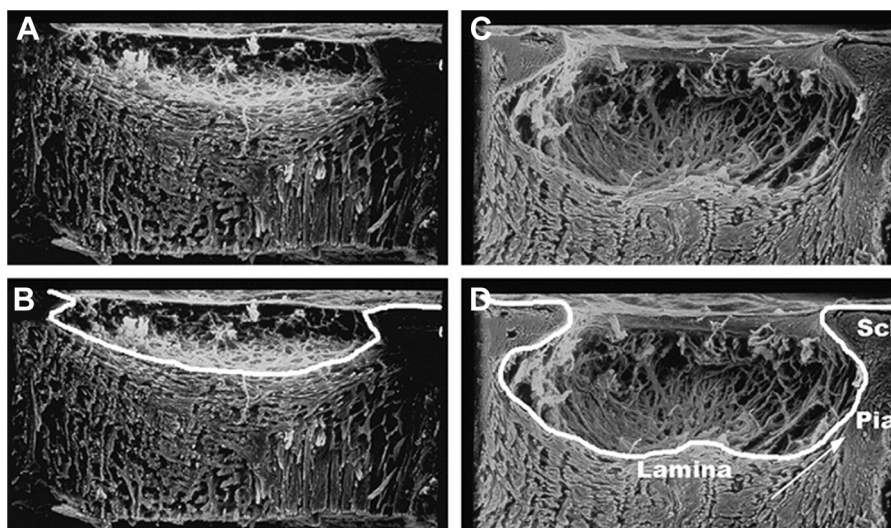


FIGURE 1. Scanning electron microscopy of the optic nerve head in human eyes. A. Normal eye. B. The same image as in panel A but with the anterior scleral canal wall and anterior lamina cribrosa surface delineated. C. Eye with glaucoma. D. The same image as in panel C but with the anterior scleral canal wall and anterior lamina cribrosa surface delineated. In most of the eyes with glaucoma, the lamina cribrosa moves backward and the anterior scleral canal expands outward compared to the normal eyes. In a certain proportion of eyes with glaucoma, however, the opposite happens, and the lamina cribrosa moves forward and the anterior scleral canal becomes smaller. This figure modifies the previously published figure in Quigley HA, Hohman RM, Addicks EM, et al. Morphologic changes in the lamina cribrosa correlated with neural loss in open-angle glaucoma. *Am J Ophthalmol* 1983;95(5); 673-691.

## METHODS

THIS CROSS-SECTIONAL STUDY WAS APPROVED BY THE institutional review and ethics boards of the Akita University Graduate School of Medicine, Akita, Japan, and carried out in accordance with the tenets of the Declaration of Helsinki. The study enrolled consecutive patients who visited the glaucoma clinic of the Akita University Graduate School of Medicine between May 2018 and May 2019. Informed consent was obtained from all participants.

The following data were collected from each patient: refraction test results, best-corrected visual acuity, central corneal thickness and axial length (SP-3000; Tomey Corporation, Nagoya, Japan), Goldmann applanation tonometry, slit-lamp biomicroscopy, gonioscopy, fundus color stereo photography (Canon, Tokyo, Japan), standard automated perimetry (Humphrey Field Analyzer II 750; 24-2 Swedish interactive threshold algorithm; Carl Zeiss Meditec, Dublin, California, USA), and SDOCT (Spectralis; Heidelberg Engineering GmbH, Heidelberg, Germany).

The SDOCT images of the ONH were acquired with the enhanced depth imaging technique, which improves visualization of the deeper structures. The radial scan SDOCT was performed from the center of the ONH and included 48 B-scan images in each eye, with each B-scan image constructed from 42 frames.<sup>8,18</sup> Magnification error was corrected using a formula provided by the manufacturer on the basis of the results of autorefraction keratometry and focus setting during image acquisition. The scaling of

the OCT images was corrected to 1:1 before evaluation. The OCT images were acquired within 3 months of the visual field (VF) test.

The study included eyes with glaucoma, which presented with glaucomatous optic disc changes such as localized or diffuse rim thinning and retinal nerve fiber layer defects, and glaucomatous VF defect corresponding to the glaucomatous structural changes. Glaucomatous VF defect was defined by glaucoma hemifield test results outside the normal range or the presence of at least 3 contiguous test points within the same hemifield on the pattern deviation plot at  $P < .05$ , with at least 1 of these points at  $P < .01$ , which was confirmed by 2 consecutive reliable tests (fixation loss rate,  $\leq 20\%$ ; false-positive and false-negative error rates,  $\leq 15\%$ ).

The exclusion criteria were as follows: (1) Eyes with myopia, with spherical equivalent  $\leq -2$  diopter and axial length  $\geq 24.0$  mm. These eyes were excluded to avoid the myopic effect on ONH deformation, because myopia is reported to cause ONH deformation by itself, including enlargement of the scleral canal and shallowing of the anterior LC depth.<sup>22,23</sup> (2) Eyes with poor-quality OCT images, defined as those with quality score  $\leq 15$ . (3) Retinal or neuro-ophthalmologic disease that might affect the VF. (4) Congenital optic disc abnormalities and suspected anomalies.<sup>24</sup> Normal eyes were included as controls when they exhibited IOP  $\leq 21$  mm Hg, open iridocorneal angle, normal-appearing optic disc, and no VF defects according to the above criteria.

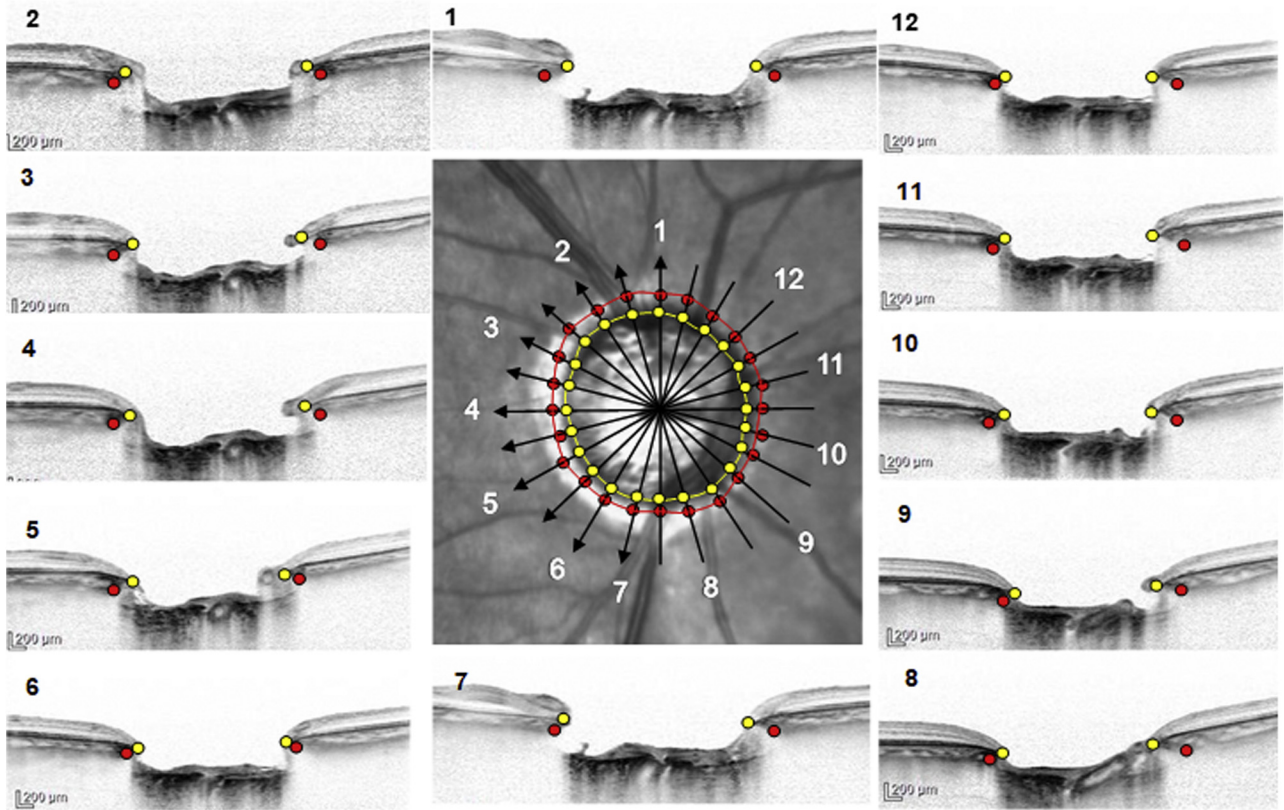


**FIGURE 2.** Delineation of the Bruch membrane (BM) opening and anterior scleral canal (ASC) opening. The central figure is an infrared (IR) fundus image of an optic disc with 12 radial scan lines of the spectral-domain optical coherence tomography. Both sides of the BM termination were detected in each B-scan image (yellow dots) and plotted on the corresponding radial scan line. The BM terminations were manually connected (yellow line in IR image), and the delineated area was defined as the BM opening. The ASC opening was obtained in the same way by delineating ASC terminations (red line in IR image).

Patients with both unilateral and bilateral glaucoma were included. The patients were diagnosed as showing unilateral glaucoma when they had glaucoma in 1 eye caused by uveitis, injury, pseudoexfoliation, or angle closure, and did not have glaucoma in the other eye. The patients with bilateral glaucoma were all primary open-angle glaucoma.

• **ASSESSMENT OF OPTIC NERVE HEAD STRUCTURES WITH SPECTRAL-DOMAIN OPTICAL COHERENCE TOMOGRAPHY:** The termination of the Bruch membrane (BM) was identified in the 12 equidistant radial SDOCT B-scans (Figure 2).<sup>8,9,25</sup> Both sides of the BM termination were plotted on the corresponding radial scan lines in the infrared (IR) fundus image on the display window of the Spectralis viewer. The 24 BM terminations plotted on the 12 radial scan lines were manually delineated, and the extent was defined as the BM opening. The ASC opening was obtained with the same method by identifying ASC terminations (Figure 3). In cases wherein the BM terminations or ASC terminations were unable to be identified in a B-scan image, the neighboring scan image was used instead.

In cases wherein they were unable to be identified in both sides of the neighboring B-scan, the eye was excluded.

Within the ONH, the cross-sectional area of the ASC was usually the smallest at its opening and larger at the deeper region close to the bottom. The largest ASC area was located somewhere between the ASC opening and anterior LC insertion. The points that showed the largest ASC area were identified in 12 equidistant radial B-scan images. They were plotted on the corresponding point on the radial scan lines in the IR fundus image and used for the measurement of the largest ASC area. The deeper structure of the ONH tended to appear blurry, and identification of the largest ASC points in all 12 radial scan lines was difficult. Therefore, we measured the largest ASC area as an ellipse that best fitted the area obtained by delineating the identifiable largest ASC points in the B-scan images.

The anterior LC depth was measured by using the sclerochoroidal junction plane as a reference to eliminate the effect of choroidal thickness.<sup>19,26</sup> The sclerochoroidal junction line was defined as the line connecting 2 points of the anterior scleral surface located at 1,750  $\mu\text{m}$  from the center of the BM opening in each B-scan line



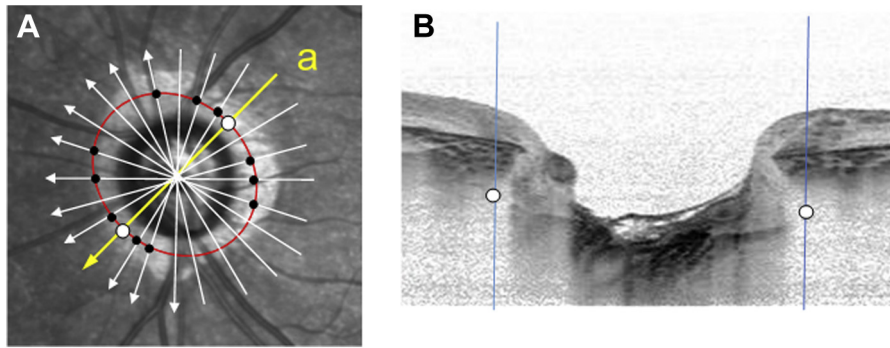


**FIGURE 3.** Measurement of the largest anterior scleral canal (ASC) area within the optic nerve head (ONH). **A.** Infrared fundus image of the ONH with 12 equidistant radial spectral-domain optical coherence tomography scan lines (white arrows). The points that showed largest ASC area within the ONH were detected in each B-scan image, and they were plotted on the corresponding location on the radial scan line (black dots). Identifying the largest ASC points in all 12 B-scan images was difficult; therefore, the largest ASC area was measured as an ellipse that best fitted to the area obtained by delineating the identifiable largest ASC points (red ellipse). **B.** B-scan image that shows largest ASC points within the ONH (white dots) that are plotted on the corresponding location in the radial scan line (line a, yellow arrow in panel A).

(Figure 4).<sup>27,28</sup> The LC depth was measured as a perpendicular distance from the reference line to the anterior LC surface at 9 points in each eye, and mean of the 9 measurements was defined as the LC depth of the eye.

- **CORRELATION BETWEEN PERCENTAGE DIFFERENCE IN THE OPTIC NERVE HEAD PARAMETERS AND DIFFERENCE IN THE VISUAL FIELD DEFECT AND INTRAOCULAR PRESSURE BETWEEN PAIRED EYES:** In patients with unilateral glaucoma, the percentage by which the ONH parameters (BM opening, ASC opening, largest ASC area, and LC depth) in the glaucomatous eye were greater than that in the fellow nonglaucomatous eye was calculated, and correlation between the percentage difference in the ONH parameters and difference in the mean deviation (MD) of the Humphrey VF test between paired eyes was examined. The association between the percentage difference of the ONH parameters and difference in the IOP (untreated IOP and IOP on the imaging day) between paired eyes was examined as well. In patients with bilateral glaucoma, the same analysis was performed between paired eyes with worse and better VF defect.

- **STATISTICAL ANALYSIS:** Differences in variables between paired eyes were assessed by paired-sample *t* test. Differences in continuous variables were assessed by Student *t* test or Mann-Whitney *U* test, depending on the normality of data distribution. Correlation between percentage difference in the ONH parameters and difference in the MD between paired eyes was assessed by Spearman rank correlation. Interobserver reproducibility of the measurements was assessed by determining the intraclass correlation coefficient (ICC) of each variable, with the corresponding 95% confidence interval (CI). The assessment was performed in 30 randomly selected subjects by 2 independent observers (Y.S. and H.S.). Statistical analysis was performed using R

software ver.3.4.2 (<https://www.r-project.org/>). Level of significance was set at  $P < .05$ . All *P* values were 2-sided.

## RESULTS

FROM THE 278 EYES OF 139 GLAUCOMA PATIENTS, 43 EYES OF 36 patients were excluded for the following reasons: poor-quality SDOCT images ( $n = 21$ ), unreliable VF test results ( $n = 10$ ), ocular diseases other than glaucoma that might affect the VF ( $n = 6$ ), and congenital optic disc anomalies or suspected anomalies ( $n = 6$ ). Both eyes of the subjects had to qualify to be included in the paired-eye study; therefore, 206 eyes of 103 patients were included in the analysis. Among these, 33 patients had unilateral glaucoma and 70 patients had bilateral glaucoma. In addition, 100 eyes of 50 normal subjects were included as controls. All the subjects were Japanese. The ICCs for the measurement of the ASC opening, largest ASC area, and LC depth were 0.89 (95% CI, 0.85-0.92), 0.82 (95% CI, 0.77-0.88), and 0.88 (95% CI, 0.83-0.94), respectively.

Among the 33 patients with unilateral glaucoma, MD of the Humphrey VF test was  $-16.35 \pm 8.87$  dB in the eyes with glaucoma and  $-0.26 \pm 1.67$  dB in the fellow normal eyes ( $P < .0001$ , Table). Untreated IOP was significantly higher in the eyes with glaucoma than in the fellow eyes, while that on the imaging day was not significantly different. The BM opening, ASC opening, largest ASC area, and LC depth were significantly greater in the eyes with glaucoma than in the fellow normal eyes (Figure 5A). Intereye differences in these parameters were significantly greater than those in normal subjects (Figure 5B). There were 6 patients who exhibited smaller BM opening in the eyes with glaucoma than in the fellow normal eyes, and 5 of them exhibited smaller ASC opening

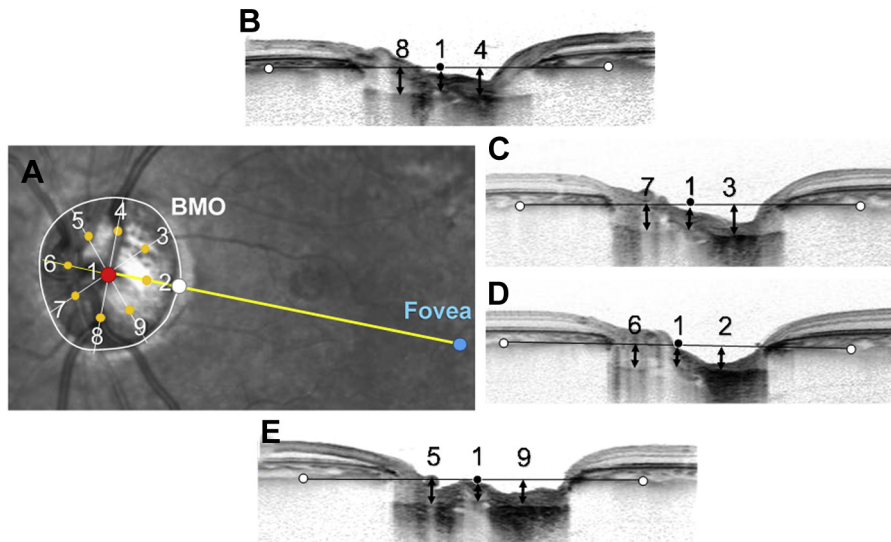


**FIGURE 4.** Measurement of the anterior lamina cribrosa (LC) depth. **A.** Infrared fundus image. The LC depth was measured at 9 points in each eye at the center of the Bruch membrane opening (BMO) (red dot, labeled as 1) and the midperipheral point of the following 8 BMO areas: temporal, supratemporal, superior, supranasal, nasal, infranasal, inferior, and infratemporal (orange dots, labeled as 2 to 9, respectively). The midperipheral point of the temporal BMO area (orange dot 2) was defined in the line that connected fovea (blue dot) and BMO center (red dot). It was defined as the central point between the BMO center (red dot) and the crossing point of the fovea–BMO center line (yellow linear line) and the BMO line (white circle line). The remaining 7 midperipheral points in each BMO area were defined in the same way in the line 45° apart from each other. **B–E.** B-scan images used for LC depth measurement. The reference line (black line) was drawn by connecting 2 terminating points of the anterior scleral surface located 1750 μm from the center of the BMO (white dots) in each B-scan, and the LC depth was measured at each midperipheral BMO point (labeled with the identical number in the infrared image) as a distance from the reference line to the anterior LC surface.

and largest ASC area in the eyes with glaucoma. There were 5 other patients who exhibited shallower LC depth in the eyes with glaucoma.

Among the 70 patients with bilateral glaucoma, when paired eyes were divided into eyes with worse and better VF defect on the basis of the MD of the Humphrey VF test, the MD was  $-16.35 \pm 8.45$  dB in the eyes with worse VF defect and  $-6.82 \pm 6.31$  dB in the eyes with better VF defect ( $P < .0001$ , Table). The BM opening, ASC opening, and largest ASC area were significantly greater in the eyes with worse VF defect than in those with better VF defect, while LC depth was not significantly different between them (Figure 6). Intereye differences in the ASC opening and largest ASC area were significantly greater than those in normal subjects (Figure 6).

In both the patients with unilateral and those with bilateral glaucoma, the percentage difference in the ONH parameters (BM opening, ASC opening, largest ASC area, and LC depth) were not significantly correlated with the MD difference or IOP difference between paired eyes after adjusting for sex and age.

## DISCUSSION

IN THE PRESENT STUDY, WE EXAMINED ASC AREA IN THE eyes with glaucoma using SDOCT. The parameters that pre-

sent ASC area (ASC opening and largest ASC area) were significantly larger in the eyes with glaucoma than in the fellow eyes without glaucoma in unilateral glaucoma patients. They were significantly larger in the eyes with worse VF than in those with better VF in bilateral glaucoma patients. To the best of our knowledge, this is the first study that demonstrated larger ASC area in the living human eyes with glaucoma compared to the normal eyes. The present study confirmed previous histologic studies that reported expansion of the ASC area in the human cadaver eyes with glaucoma and animal experimental glaucoma.<sup>1,2,6,10,12</sup>

The present study demonstrated significantly larger ASC area in the eyes with glaucoma than in the fellow eyes in unilateral glaucoma, and in the eyes with worse VF than in those with better VF in bilateral glaucoma. There may be several explanations for these results. One is that the ASC area expanded during the course of glaucoma. In this case, the large ASC area was considered to be the consequence of the glaucomatous ONH deformation, and the ASC area may be useful in the treatment of glaucoma by monitoring development and progression of the disease. The other possible explanation is that the eyes that originally had large ASC area possessed susceptibility to the glaucomatous stress, and they developed glaucoma later. In this case, the large ASC area is considered to be the cause of glaucoma. The ASC area may predict risk of the

**TABLE. Demographic Data of the Participants**

	Paired Eyes With Unilateral Glaucoma With and Without Glaucoma (N = 33)		Paired Eyes With Bilateral Glaucoma With Worse and Better VFD (N = 70)		Normal Subjects (N = 50)		
	Eyes With Glaucoma	Eyes Without Glaucoma	Eyes With Worse VFD	Eyes With Better VFD	Right Eyes	Left Eyes	
			P Values <sup>a</sup>		P Values <sup>a</sup>		P Values <sup>a</sup>
Sex (male/female)	17/16				23/27		
Age (y)	67.4 ± 11.8				68.2 ± 8.7		
Mean deviation (decibel)	-16.35 ± 8.87	-0.26 ± 1.67	<.0001*	-6.82 ± 6.31	-0.15 ± 1.23	-0.23 ± 1.43	.5348
IOP: untreated (mm Hg)	37.0 ± 13.4	17.0 ± 3.7	<.0001*	20.1 ± 6.6	n/a	n/a	n/a
IOP: imaging day (mm Hg)	16.4 ± 5.8	14.6 ± 3.7	.0756	15.0 ± 4.0	14.0 ± 3.1	14.0 ± 2.8	1.0000
Spherical equivalent (diopter)	0.25 ± 1.29	0.13 ± 1.37	.2217	0.33 ± 1.09	0.22 ± 1.08	0.30 ± 1.32	.6021
Axial length (mm)	23.18 ± 0.94	23.16 ± 0.91	.6185	23.11 ± 0.69	23.07 ± 0.72	23.06 ± 0.74	.7341
Central corneal thickness (μm)	523.6 ± 28.4	532.5 ± 28.3	.0048*	512.8 ± 35.6	512.6 ± 35.6	552.4 ± 40.0	.1159

IOP = intraocular pressure; VFD = visual field defect. Values are shown in means ± standard deviations. Asterisk (\*) indicates statistical significance. <sup>a</sup>Paired-sample t test.

development of glaucoma, and it may be useful in the prevention of the disease. This is a cross-sectional study, and the causal relationship between the large ASC area and glaucoma development is unknown. Further longitudinal studies are required to determine it.

In the present study, the difference of the ONH parameters between paired eyes were not significantly associated with the difference of the IOP between them. The IOP is known to be a factor that affects ONH morphology.<sup>3,4,8,9,13-16</sup> The present study took only the untreated IOP and IOP on the imaging day into consideration; however, they might not be enough to evaluate its effect on the ONH morphology, and other IOP-related parameters such as the time course of IOP and its fluctuation might be needed to evaluate its effect more accurately.<sup>29,30</sup> Alternatively, the association between the IOP and ONH deformation in glaucoma may not be simple but rather complex. In the present study, most of the patients with unilateral glaucoma exhibited larger ASC area and deeper LC depth in the eyes with glaucoma than in the fellow normal eyes; however, a certain proportion of them exhibited opposite deformations. The deformation of the ASC and LC may interact, and its magnitude is dependent on the level of IOP and the shape and stiffness of each tissue. A more compliant sclera will expand more, and the lamina will be pulled taut and displace anteriorly. A less compliant sclera will expand less, and the lamina will displace posteriorly. Further studies are needed to evaluate association between IOP and ONH deformation in glaucoma.

In the present study, the LC depth was significantly greater in the eyes with glaucoma than in the fellow eyes without glaucoma in patients with unilateral glaucoma, which is in line with previous studies that reported posterior displacement of the LC in glaucoma eyes compared to the normal eyes.<sup>7</sup> In the patients with bilateral glaucoma, however, the LC depth was not significantly deeper in the eyes with worse VF than in those with better VF. A previous study investigated LC depth in different stages of glaucoma, and reported that the LC depth was significantly greater in the eyes with mild-to-moderate VF defect than in those with preperimetric and early stages of glaucoma; however, it was not significantly different between eyes with mild-to-moderate and severe VF defect.<sup>31</sup> The present study is in line with the previous study, and suggested that posterior displacement of the LC may occur mostly in the preperimetric to early stage of glaucoma, and it may stabilize after that stage. The alteration of the LC position during the course of glaucoma requires further investigation.

The present study used paired-eye comparison to evaluate influence of glaucoma on the ONH deformation, and this was considered to be effective in eliminating the influence of other systemic factors including aging.<sup>25,32</sup> Since tissue loses its compliance with aging,<sup>33</sup> and deformation of the ONH structure is largely affected by the stiffness of the tissue,<sup>13-16</sup> the optic discs in elderly eyes with stiffer

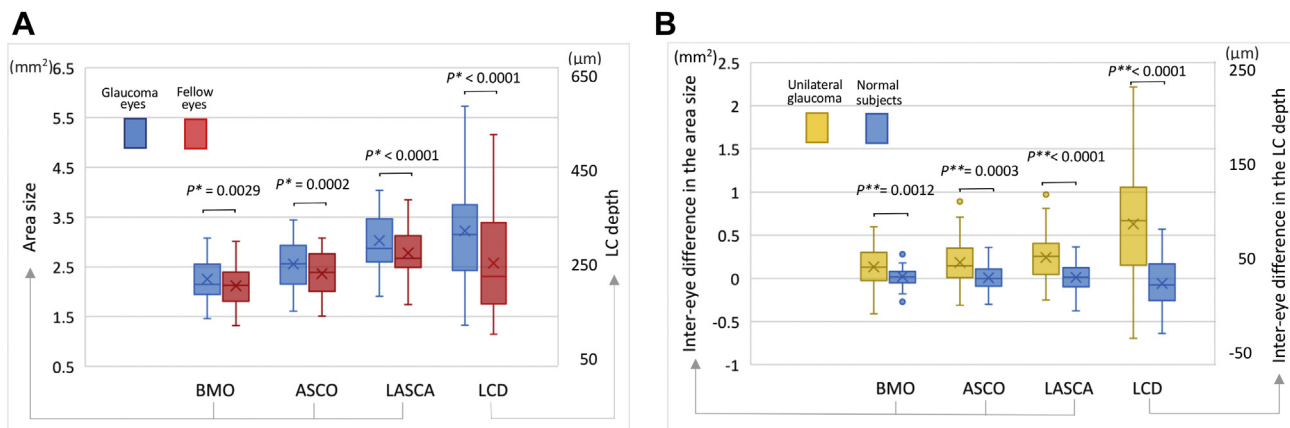


**FIGURE 5.** Comparison of the optic nerve head (ONH) parameters between paired eyes in patients with unilateral glaucoma. **A.** Comparison of the ONH parameters between eyes with glaucoma and fellow normal eyes. **B.** Comparison of the intereye difference of the ONH parameters between patients with unilateral glaucoma and normal subjects. \*Paired-sample *t* test. \*\*Student *t* test. ASCO = anterior scleral canal opening; BMO = Bruch membrane opening; LASCA = largest anterior scleral canal area; LCD = lamina cribrosa depth.

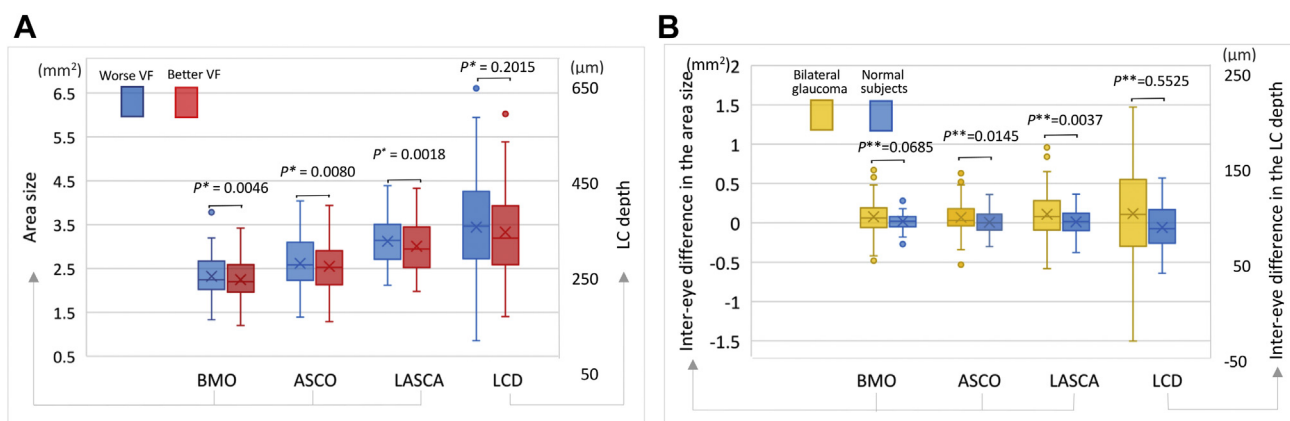


**FIGURE 6.** Comparison of the optic nerve head (ONH) parameters between paired eyes with worse and better visual field (VF) defect in patients with bilateral glaucoma. **A.** Comparison of the ONH parameters between paired eyes with worse and better VF defect. **B.** Comparison of the intereye difference of the ONH parameters between patients with bilateral glaucoma and normal subjects. \*Paired-sample *t* test. \*\*Student *t* test. ASCO = anterior scleral canal opening; BMO = Bruch membrane opening; LASCA = largest anterior scleral canal area; LCD = lamina cribrosa depth; VF = visual field.

tissue tend to exhibit less deformation than that in the younger eyes with more compliant tissue with similar levels of VF defect.<sup>34</sup> The 2 eyes of the same individual are supposed to have the same effect of aging; therefore, a paired-eye comparison should be effective in eliminating the influence of aging from our results. In addition, this approach was thought to be effective in minimizing the influence of variation of the ONH structure among individuals, since paired eyes are reported to exhibit similar disc morphology.<sup>35</sup>

The percentage difference in the ONH parameters (BM opening, ASC opening, largest ASC area, and LC depth) between paired eyes was not significantly correlated with

the MD difference between them in either unilateral or bilateral glaucoma patients. It indicated that although ONH deformation may contribute to creating glaucomatous VF defect, the magnitude of ONH deformation was not linearly correlated with the severity of the VF defect. These results are in accordance with those of the previous studies that reported insignificant correlation between parameters of ONH deformation and axonal count in animal experimental glaucoma.<sup>33,36,37</sup> The authors suggested that although global ONH deformation is related to the retinal ganglion cell axonal loss, it does not explain glaucomatous axonal loss all by itself, and microstructural change in the LC and underlying cellular mechanism may play an



important role in it. This would explain the current results obtained in the living human eyes with glaucoma as well.

The present study has several limitations. First, the visibility of the deep ONH structure was not always clear, even with the use of enhanced depth imaging technique, and reproducibility of the data was not sufficient enough, particularly for the largest ASC area (ICC, 0.82, 95% CI, 0.77-0.88). Therefore, the detection of the difference of the parameters might be difficult particularly when the difference was small. This is considered to be the limitation of the OCT device we currently use, and invention of an OCT that allows better visibility of the deeper structure is required. Second, there was a considerable amount of overlap in the measured ONH parameters between paired eyes, and even though there was a statistically significant difference between them, the actual difference was small. Therefore, caution is required in the interpretation of the results. Third, the LC depth was measured at the central and midperipheral optic disc areas but not at the peripheral area; therefore, this approach might not reveal LC depth accurately. The depth was not measured at the peripheral area, because it was not reliable under the thick overlying tissues. The present study aimed not to provide accurate LC depth, but to compare it between paired eyes under the same condition. Considering similar optic disc shape and size between paired eyes,<sup>35</sup> the LC depth was supposed to be measured at similar disc locations between them; therefore, we believe our method was able to capture the difference of the LC depth between paired eyes and provided enough data for our purpose. Finally, ASC area was measured in 2-dimensional images using IR images, and it

might be more accurate if it was measured in 3-dimensional images considering tilt of the optic disc that includes deformation in the z-axis direction. We do not have access to the engineering 3-dimensional quantification of the ONH structure in our institute; therefore, we excluded myopic eyes that often present tilted disc from the subject, which was supposed to be effective in minimizing the influence of distortion of the ASC area.

In conclusion, ASC area was significantly larger in the living human eyes with glaucoma compared to the normal eyes using SDOCT. Further longitudinal studies are required to determine if the ASC area is useful in monitoring development and progression of the ONH deformation in glaucoma or in predicting susceptibility to the glaucoma stress.

---

## CRediT AUTHORSHIP CONTRIBUTION STATEMENT

**YU SAWADA:** CONCEPTUALIZATION, METHODOLOGY, Validation, Formal analysis, Investigation, Resources, Data curation, Writing - original draft, Writing - review & editing, Visualization, Project administration, Funding acquisition. **Makoto Araie:** Writing - original draft, Writing - review & editing, Supervision. **Hitomi Shibata:** Validation, Investigation, Resources. **Katsuyuki Murata:** Formal analysis. **Makoto Ishikawa:** Resources. **Takeshi Yoshitomi:** Supervision. **Takeshi Iwase:** Supervision, Project administration.

---

FUNDING/SUPPORT: THIS STUDY IS SUPPORTED BY A GRANT FROM THE JAPAN SOCIETY FOR THE PROMOTION OF SCIENCE (JSPS) (Number; 17K11417), Tokyo, Japan. The funding organization had no role in the design or conduct of this research.

Financial Disclosures: The following authors have no financial disclosures: Yu Sawada, Makoto Araie, Hitomi Shibata, Makoto Ishikawa, Katsuyuki Murata, Takeshi Yoshitomi, and Takeshi Iwase. All authors attest that they meet the current ICMJE criteria for authorship.

---

## REFERENCES

1. Quigley HA, Hohman RM, Addicks EM, Massof RW, Green WR. Morphologic changes in the lamina cribrosa correlated with neural loss in open-angle glaucoma. *Am J Ophthalmol* 1983;95(5):673-691.
2. Pederson JE, Anderson DR. The mode of progressive disc cupping in ocular hypertension and glaucoma. *Arch Ophthalmol* 1980;98(3):490-495.
3. Burgoyne CE. The non-human primate experimental glaucoma model. *Exp Eye Res* 2015;141:57-73.
4. Yang H, Reynaud J, Lockwood H, et al. The connective tissue phenotype of glaucomatous cupping in the monkey eye—clinical and research implications. *Prog Retin Eye Res* 2017; 59:1-52.
5. Quigley HA, Addicks EM, Green WR, Maumenee AE. Optic nerve damage in human glaucoma II. The site of injury and susceptibility to damage. *Arch Ophthalmol* 1981;99(4):635-649.
6. Quigley HA, Green WR. The histology of human glaucoma cupping and optic nerve damage: clinicopathologic correlation in 21 eyes. *Ophthalmology* 1979;86:1803-1830.
7. Furlanetto RL, Park SC, Damle UJ, et al. Posterior displacement of the lamina cribrosa in glaucoma: in vivo interindividual and intereye comparisons. *Invest Ophthalmol Vis Sci* 2013;54(7):4836-4842.
8. Lee EJ, Kim TW, Weinreb RN. Reversal of lamina cribrosa displacement and thickness after trabeculectomy in glaucoma. *Ophthalmology* 2012;119:1359-1366.
9. Lee EJ, Kim TW. Lamina cribrosa reversal after trabeculectomy and the rate of progressive retinal nerve fiber layer thinning. *Ophthalmology* 2015;122:2234-2242.
10. Downs JC, Yang H, Girkin C, et al. Three-dimensional histomorphometry of the normal and early glaucomatous monkey optic nerve head: neural canal and subarachnoid space architecture. *Invest Ophthalmol Vis Sci* 2007;48(7): 3195-3208.



11. Burgoyne CF, Downs JC, Bellezza AJ, Hart RT. Three-dimensional reconstruction of normal and early glaucoma monkey optic nerve head connective tissues. *Invest Ophthalmol Vis Sci* 2004;45(12):4388–4399.
12. Yang H, Downs JC, Girkin C, et al. 3D histomorphometry of the normal and early glaucomatous monkey optic nerve head: lamina cribrosa and peripapillary scleral position and thickness. *Invest Ophthalmol Vis Sci* 2007;48(10):4597–4607.
13. Sigal IA, Flanagan JG, Tertinegg I, Ethier CR. 3D morphometry of the human optic nerve head. *Exp Eye Res* 2010;90:70–80.
14. Bellezza AJ, Hart RT, Burgoyne CF. The optic nerve head as a biomechanical structure: initial finite element modeling. *Invest Ophthalmol Vis Sci* 2000;41(2):2991–3000.
15. Sigal IA, Yang H, Roberts MD, Burgoyne CF, Downs JC. IOP-induced lamina cribrosa displacement and scleral canal expansion: an analysis of factors interactions using parameterized eye-specific models. *Invest Ophthalmol Vis Sci* 2011;52(3):1896–1907.
16. Sigal IA, Flanagan JG, Tertinegg I, Ethier CR. Modeling individual-specific human optic nerve head biomechanics. Part 2: influence of material properties. *Biomech Model Mechanobiol* 2009;8(2):99–109.
17. Inoue R, Hangai M, Kotera Y, et al. Three dimensional high-speed optical coherence tomography imaging of lamina cribrosa in glaucoma. *Ophthalmology* 2009;116:214–222.
18. Lee EJ, Kim TW, Weinreb RN, Park KH, Kim SH, Kim DM. Visualization of the lamina cribrosa using enhanced depth imaging spectral-domain optical coherence tomography. *Am J Ophthalmol* 2011;152(1):87–95.
19. Vianna JR, Lanoe VR, Quach J, et al. Serial changes in lamina cribrosa depth and neuroretinal parameters in glaucoma: impact of choroidal thickness. *Ophthalmology* 2017;124:1392–1402.
20. Yang H, Luo H, Gardiner SK, et al. Factors influencing optical coherence tomography peripapillary choroidal thickness: a multicenter study. *Invest Ophthalmol Vis Sci* 2019;60(2):795–806.
21. Luo H, Yang H, Gardiner SK, et al. Factors influencing central lamina cribrosa depth: a multicenter study. *Invest Ophthalmol Vis Sci* 2018;59(6):2357–2370.
22. Ramrattan RS, Wolfs RC, Jonas JB, Hofman A, de Jong PT. Determinations of optic disc characteristics in a general population: the Rotterdam study. *Ophthalmology* 1999;106:1588–1596.
23. Jonas JB, Gusek GC, Naumann GO. Optic disc morphometry in high myopia. *Graefes Arch Clin Exp Ophthalmol* 1988;226(6):587–590.
24. Apple DJ, Rabb MF, Walsh PM. Congenital anomalies of the optic disc. *Surv Ophthalmol* 1982;27(1):3–41.
25. Sawada Y, Hangai M, Ishikawa M, Yoshitomi T. Association of myopic deformation of optic discs with visual field progression in paired eyes with open-angle glaucoma. *PLoS One* 2017;12:e0170733.
26. Moghimi S, Nekoozadeh S, Motamed-Gorji N, et al. Lamina cribrosa and choroid features and their relationship to stage of pseudoexfoliation glaucoma. *Invest Ophthalmol Vis Sci* 2018;59(13):5355–5363.
27. Johnstone J, Fazio M, Rojananuangnit K, et al. Variation of the axial location of Bruch's membrane opening with age, choroidal thickness, and race. *Invest Ophthalmol Vis Sci* 2014;55(3):2004–2009.
28. Sawada Y, Hangai M, Murata K, et al. Lamina cribrosa depth variation measured by spectral-domain optical coherence tomography within and between four glaucomatous optic disc phenotypes. *Invest Ophthalmol Vis Sci* 2015;56(10):5777–5784.
29. Baskaran M, Kumar RS, Govindasamy CV, et al. Diurnal intraocular pressure fluctuation and associated risk factors in eyes with angle closure. *Ophthalmology* 2009;116:2300–2304.
30. De Moraes CG, Jasien JV, Simon-Zoula S, Liebman JM, Ritch R. Visual field and 24-hour IOP-related profile with a contact lens sensor in treated glaucoma patients. *Ophthalmology* 2016;123:744–753.
31. Park SC, Brumm J, Furlanetto RL, et al. Lamina cribrosa depth in different stages of glaucoma. *Invest Ophthalmol Vis Sci* 2015;56(3):2059–2064.
32. Kim DW, Jeoung JW, Kim YW, et al. Prelamina and lamina cribrosa in glaucoma patients with unilateral visual field loss. *Invest Ophthalmol Vis Sci* 2016;57(4):1662–1670.
33. Burgoyne CF, Downs JC. Premise and prediction - how optic nerve head biomechanics underlies the susceptibility and clinical behavior of the aged optic nerve head. *J Glaucoma* 2008;17(4):318–328.
34. Ren R, Yang H, Gardiner SK, et al. Anterior lamina cribrosa surface depth, age and visual field sensitivity in the Portland progression project. *Invest Ophthalmol Vis Sci* 2014;55(3):1531–1539.
35. Sawada Y, Ishikawa M, Sato N, Yoshitomi T. Optic nerve head morphology assessed by laser scanning tomography in normal Japanese subjects. *J Glaucoma* 2011;20(7):445–451.
36. Yang H, Ren R, Lockwood H, et al. The connective tissue components of optic nerve cupping in monkey experimental glaucoma part 1: global change. *Invest Ophthalmol Vis Sci* 2015;56(13):7661–7678.
37. Tan JC, Kalapesi FB, Coroneo MT. Mechanosensitivity and the eye: cells coping with the pressure. *Br J Ophthalmol* 2006;90(3):383–388.